Multiscale classification of very high resolution SAR images of urban areas by Markov random fields, copula functions, and texture extraction

Aurélie Voisin, Vladimir Krylov, Gabriele Moser, Sebastiano B. Serpico, Josiane Zerubia

MULTISCALE CLASSIFICATION OF VERY HIGH RESOLUTION SAR IMAGES OF URBAN AREAS BY MARKOV RANDOM FIELDS, COPULA FUNCTIONS, AND TEXTURE EXTRACTION

Aurélie Voisin[†]*, Vladimir A. Krylov*[†]*, Gabriele Moser*[*]*, Sebastiano B. Serpico*[*]*, and Josiane Zerubia*[†]

[*] University of Genoa, I-16145, Genoa, Italy, [name.surname]@unige.it
[†] Ayin team, INRIA, F-06902, Sophia Antipolis Cedex, France, [name.surname]@inria.fr

ABSTRACT

This paper addresses the problem of classifying very high resolution synthetic aperture radar (SAR) images of urban areas by using a supervised Bayesian classification method via a contextual hierarchical approach. We develop a bivariate copula-based statistical model that combines amplitude SAR data and textural information. This model is plugged into a hierarchical Markov random field based on a quadtree structure and on multiscale wavelet features. The contribution of this paper is thus the development of a novel hierarchical classification approach that uses a quadtree model based on the wavelet decomposition and an innovative statistical model. The performance of the developed approach is illustrated on a COSMO-SkyMed image of a urban area.

1. INTRODUCTION

Synthetic aperture radar (SAR) is an active image acquisition system which allows day-and-night and all-weather acquisitions [15]. Such properties are crucial, for example, for risk management applications, allowing land-use and land cover mapping, as well as the detection of areas damaged by natural disasters such as earthquakes or floods. In this letter we address the problem of classifying very high resolution (VHR) SAR images of urban areas, that represents an especially interesting typology in important applications such as civil protection for disaster monitoring and damage assessment. This interest is further enforced by the current availability of VHR satellite SAR data collected by the COSMO-SkyMed and TerraSAR-X missions.

Nevertheless, several difficulties have to be considered to address the VHR SAR classification problem. The first one is related to the inherent multiplicative noise known as speckle, which originates from the interference of the coherent wavefronts. This type of noise is specific to active imaging systems and degrades appreciably the recorded imagery [15]. As a consequence, standard classification methods that have been validated for optical data, do not report satisfying results when applied directly to SAR images. Another difficulty is the heterogeneity of urban areas in VHR images, that leads to heterogeneous statistical modeling, reflecting the different ground materials such as asphalt, concrete, metal, etc. A variety of supervised methods have been considered in the literature for SAR image classification, including active contours [16], bags-of-words [5], rule-based methods [4], etc.

In this paper we propose a statistical Bayesian supervised classification approach that consists of two steps. The first step deals with modeling the SAR amplitude statistics conditioned to each target class (e.g. vegetation, urban, etc.) by using finite mixtures of automatically chosen SAR-specific probability density functions (PDFs) [13], that are intended to take into account the above mentioned heterogeneity of VHR SAR statistics. We further consider an additional source of information obtained by extracting a textural feature map from the original SAR image in order to optimize the detection of urban areas or, more generally, of highly textured classes. The estimates of the marginal PDFs of the original SAR image and the textural feature are combined via copulas, leading to a joint PDF estimate for each class. Copula functions represent a general a flexible tool to model the dependence among multiple random variables whose marginal PDFs are known or can be separately estimated [14]. The use of copulas in the proposed method is explained by the lack of accurate parametric models for the joint statistics of SAR amplitude and texture features.

In the second step of the proposed technique, a classification map is generated by using the resulting copula-based estimates of the class-conditional statistics. To improve robustness against speckle, we consider a contextual model based on a multiscale Markov random field (MRF) [7]. MRFs represent a general family of powerful stochastic models for the spatial context associated with image data in Bayesian image processing [6]. Multiscale approaches currently play a primary role in VHR image analysis. They extract both coarse-scale features, characterizing the largest structures in the image with strong immunity to speckle, and fine-scale features, detecting also smaller structures and spatial details, albeit with stronger sensitivity to speckle. Wavelet transforms [12] are used in the proposed method to generate multiscale features and a hierarchical MRF-based approach is defined to fuse the extracted multiscale information and generate the output

classification map.

The novel contribution of this paper is twofold. First, we propose a joint amplitude-texture PDF modeling that aims to help discriminating urban areas in VHR imagery. Then, we integrate this joint PDF model into a hierarchical MRF into which we introduce an algorithm to iteratively update prior-probability estimates. This algorithm experimentally leads to improved results that are less affected by speckle noise as compared to the use of a predefined prior [11].

The paper is organized as follows. In Sec. 2, we introduce the statistical bivariate copula-based model that combines marginal PDF models for SAR amplitude data and their spatial texture. In Sec. 3, we develop an MRF-based classification technique, based on the approach of the maximization of posterior marginals (MPM), on a quad-tree multiscale lattice, and on the aforementioned prior update. In Sec. 4, we present the classification results obtained from a VHR COSMO-SkyMed image. Finally, in Sec. 5, we draw conclusions.

2. JOINT AMPLITUDE-TEXTURE PDF MODEL

To construct a classification algorithm that can effectively discriminate also urban areas, we propose to extract additional textural information from the original SAR image. For this purpose, the class-conditional marginal statistics of the SAR image and its textural feature are separately modeled and then gathered into a joint amplitude-texture PDF estimate by using the statistical tool of copulas.

2.1. Textural features

Well-chosen textural features often turn out to be discriminative with respect to urban areas imaged by VHR sensors. Taking into account this information is helpful when classifying such areas. Here, motivated by the experimental textural feature extraction study performed in [18], we consider a feature obtained by the method of the greylevel co-occurrence matrix (GLCM), which characterizes the joint statistics of the greylevels of different pixels as a function of their reciprocal spatial locations [8]. Typically, the (i, j)-th entry of the GLCM is an estimate of the probability that a pixel with greylevel i is adjacent, in a given direction and with a given spatial offset, to a pixel with greylevel j. Here, we consider horizontal adjacency with a unitary offset, i.e the GLCM is computed by considering a reference pixel and the pixel located to its right. Among various texture features that can be extracted from the GLCM, we use the variance, which well discriminates the urban areas, as confirmed by our previous experiments with single-scale classification of VHR SAR images [18]. Nevertheless, it is worth noting that the proposed method can be applied with an arbitrary choice of the texture feature. This approach to texture extraction is applied on a moving-window basis, meaning that each pixel of the image successively becomes the central pixel of the window, and its value is replaced by the variance value estimated within the window.

2.2. Combined amplitude-texture model

We now present the procedures proposed for estimating the marginal class-conditional statistics and the joint amplitude-texture PDF $p_m(y|\omega_m)$. Here, $y = (y_1, y_2)$ denote the SAR amplitude y_1 of a generic pixel and its corresponding textural feature y_2, both modeled as continuous random variables; ω_m is the m-th class considered for classification and endowed with training samples ($m = 1, 2, \ldots, M$).

2.2.1. Marginal PDF estimation

For each feature y_j (either SAR amplitude or texture) and each class ω_m, the marginal PDF $p_{mj}(y_j|\omega_m)$ is modeled as a finite mixture, i.e. ($j = 1, 2; m = 1, 2, \ldots, M$):

$$p_{mj}(y_j|\omega_m) = \sum_{i=1}^{K_{mj}} P_{mij} p_{mij}(y_j|\theta_{mij}), \qquad (1)$$

where K_{mj} is the number of mixture components, $\{P_{mij} : i = 1, 2, \ldots, K_{mj}\}$ is the set of mixing proportions ($0 \leq P_{mij} \leq 1$ and $\sum_i P_{mij} = 1$), $p_{mij}(\cdot)$ is the i-th mixture component, and θ_{mij} is the vector of the parameters of this component. The use of a finite mixture model instead of a single parametric model allows capturing the behaviors of heterogeneous PDFs, which usually reflects the presence of multiple ground materials that can be appreciated for each land-cover class (e.g., different kinds of crops for the vegetation class). Such class heterogeneity is especially relevant because we deal with VHR images of urban areas [13].

For each class ω_m and each feature y_j ($j = 1, 2; m = 1, 2, \ldots, M$), each mixture component $p_{mij}(\cdot)$ ($i = 1, 2, \ldots, K_{mj}$) is automatically chosen in a predefined dictionary including the four following distributions: log-Normal, Weibull, Nakagami, and Generalized Gamma. For each class and feature, this strategy prevents the need to manually choose a given parametric model and allows the selection of a suitable model, drawn from the dictionary, to be automated. Specifically, this automatic selection, the estimation of the parameter vectors θ_{mij} ($i = 1, 2, \ldots, K_{mj}$), and the optimization of the number K_{mj} of components are jointly addressed by applying to the training samples of ω_m the algorithm in [13] and [10], that combines the approaches to PDF estimation based on the stochastic expectation maximization and on the method of log-cumulants. Details on this approach can be found in [10]. This algorithm was initially developed for SAR amplitude data, but the high flexibility of finite mixture models allows the use of this technique to be extended also to the extracted textural feature. Also in this application to textures, we empirically observed the high estimation quality of this approach.

2.2.2. Copula-based joint PDF estimation

Given the marginal PDF estimates obtained as in the previous section, the use of copula functions allows modeling the joint class-conditional PDFs of the amplitude and texture features. Also in this case, a dictionary-based approach is used by fitting several dependence structures and selecting the best fit.

A bivariate copula is a two-dimensional joint cumulative distribution function (CDF) defined on $[0,1]^2$ and such that the related marginal distributions are uniform on $[0,1]$. The importance of copula functions essentially derives from Sklar's theorem that states that, for any pair (u,v) of random variables, there exists a copula C such that the joint CDF of u and v can be expressed as:

$$F_{uv}(u,v) = C\left[F_u(u), F_v(v)\right], \tag{2}$$

where F_u and F_v are the marginal CDFs of u and v, respectively. Furthermore, if u and v are continuous random variables, C is also unique [14].

Accordingly, for each class ω_m, a unique copula C_m exists such that the joint PDF $p_m(y|\omega_m)$ of y_1 and y_2 conditioned to ω_m is expressed as ($m = 1,2,\ldots,M$):

$$\begin{aligned} p_m(y_1,y_2|\omega_m) &= p_{m1}(y_1|\omega_m)p_{m2}(y_2|\omega_m)\cdot \\ &\quad \cdot c_m\left[F_{m1}(y_1|\omega_m), F_{m2}(y_2|\omega_m)\right], \end{aligned} \tag{3}$$

where $p_{mj}(y_j|\omega_m)$ is the marginal PDF of the j-th feature ($j = 1,2$), estimated as in Sec. 2.2.1, $F_{mj}(y_j|\omega_m)$ is the corresponding marginal CDF, and:

$$c_m(u,v) = \frac{\partial^2 C_m(u,v)}{\partial u \partial v} \tag{4}$$

for almost every $(u,v) \in [0,1]^2$.

Hence, for each class ω_m, the estimation of the joint PDF $p_m(y|\omega_m)$ boils down to the determination of the copula C_m involved in Eqs. (3) and (4) ($m = 1,2,\ldots,M$). For this purpose, the method proposed in [10] is applied. In this method, a dictionary of five parametric copulas is considered: Clayton, Ali-Mikhail-Haq, Frank, Marchal-Olkin and Farlie-Gumbel-Morgenstern [14]. This choice of copulas is somewhat arbitrary, but is capable of modeling a wide variety of dependence structures [9, 14]. This set of copulas can be adjusted to fit specific classes for a given application. We refer to [14] for details on each copula function included in the dictionary and for its analytical expression. Here, we only recall that each considered parametric copula involves only one scalar parameter. To estimate this parameter, we use the relationship between copulas and Kendall's τ, which is a concordance-discordance statistics that can be empirically estimated by using the training samples of ω_m [14]. Then, for each class ω_m, the best fitting copula is chosen within the dictionary according to the highest p-value reported by the Pearson chi-square goodness-of-fit test ($m = 1,2,\ldots,M$). Details on this procedure can be found in [10].

3. PROPOSED HIERARCHICAL CLASSIFICATION APPROACH

3.1. Hierarchical multiscale model

Let a VHR SAR amplitude image and a set $\Omega = \{\omega_m\}_{m=1}^M$ of classes, each characterized by training pixels, be given. In order to generate a classification map for the considered image, a multiscale approach is adopted, in which additional features associated with different spatial scales are extracted and jointly used for classification purposes. To this end, an R-level two-dimensional decimated discrete wavelet decomposition is applied [12]. The related approximation coefficients at each n-th scale ($n = 1,2,\ldots,R$) and the original SAR amplitude image, which plays the role of the "0-th scale," represent the extracted multiscale features. As n increases in $[0,R]$, features associated with progressively coarser spatial details are considered. At each level, a texture feature is also computed through the GLCM approach (see Sec. 2.1) from the corresponding image in the decomposition stack. Hence, bivariate data are obtained at each n-th level ($n = 0,1,\ldots,R$). This multiscale approach favors robustness against speckle and allows taking benefit of the high spatial resolution of the input SAR image [17].

To formalize the classification problem, we propose to employ an explicit hierarchical graph-based model [11]. According to the aforementioned decimated wavelet approach, we shall focus on specific graphs, which have a quadtree structure (see Fig. 1). Therefore, the set S of sites is hierarchically partitioned on $S = S^0 \cup S^1 \cup \ldots \cup S^R$, where R corresponds to the coarsest resolution (i.e., the root of the quadtree), and 0 is the reference level (finest resolution). A class label x_s and an observation vector y_s ($x_s \in \Omega, y_s \in \mathbb{R}^2$) are associated with each site $s \in S$. We aim at estimating the set of hidden labels $X = \{x_s\}_{s\in S}$ given the set of observations $Y = \{y_s\}_{s\in S}$. X and Y are considered to be random processes and X is modeled as a hierarchical MRF. This implies that the strict positivity condition $P(X) > 0$ holds for the joint distribution of the class labels [6] and that Markovianity is assumed to hold both spatially and with respect to scale [11], i.e., a neighborhood system is supposed to be defined on the site lattice S^n associated with each scale $n = 0,1,\ldots,R$ and:

- The following scale-Markovianity condition holds for $n < R$:

$$P(X^n|X^k, k > n) = P(X^n|X^{n+1}), \tag{5}$$

  where $X^n = \{x_s\}_{s\in S^n}$ denotes the set of class labels associated with the n-the scale.

- The following spatial Markovianity condition holds for each scale level and each site $s \in S^n$:

$$P(x_s|x_t, t \in S^n, t \neq s) = P(x_s|x_t, t \in S^n, t \sim s), \tag{6}$$

where $t \sim s$ indicates that sites s and t ($s, t \in S^n$) are neighbors with respect to the neighborhood system on S^n.

Using a quad-tree allows taking benefit from its good properties (e.g., causality) and applying non-iterative algorithms, thus resulting in a computational time decrease as compared to iterative optimization procedures over graphs. Among the different algorithms proposed in the literature to estimate the label field X from the observation field Y, a first option is to search for an exact maximum *a-posteriori* (MAP) estimate. However, this criterion is known to be affected by critical underflow problems associated with very small probability values [11]. Therefore, as an alternate approach, we adopt the MPM criterion, that searches for an exact estimator of the marginal posterior mode of the distribution of X conditioned to Y [11]. The cost function associated with this estimator offers the possibility to penalize the errors according to their number and to the scale of the quadtree at which they occur: for example, an error at the coarsest scale is more strongly penalized than an error at the finest scale.

3.2. Multiscale MPM formulation

For each site $s \in S^n$ at each level $n = 1, 2, \ldots, R-1$ of the quadtree, a unique parent site $s^- \in S^{n+1}$ and four children sites, collected in the set $s^+ \subset S^{n-1}$ are well defined (see Fig. 1(a)). Obviously, a site at the 0-th scale has a parent but no children and a site at the R-th scale has four children but no parent. The aim of the MPM approach is to maximize the posterior marginal probability distribution $P(x_s|Y)$ at each site $s \in S$. A classical MPM algorithm is generally run in two passes, referred to as bottom-up ("forward") and top-down ("backward") passes [11]. The bottom-up pass estimates the partial posterior marginals $P(x_s|y_{d(s)})$, where $y_{d(s)}$ denotes the collection of the observations of all quadtree sites that are descendants of site s. The top-down pass estimates the labels at each tree level by maximizing the posterior marginals $P(x_s|Y)$.

Concerning the former step, Laferte et al. proved that [11]:

$$P(x_s|y_{d(s)}) \propto p(y_s|x_s)P(x_s) \cdot \cdot \prod_{t \in s^+} \sum_{x_t \in \Omega} \frac{P(x_t|y_{d(t)})P(x_t|x_s)}{P(x_t)}. \quad (7)$$

Thus, the bottom-up pass is a recursion that estimates $P(x_s|y_{d(s)})$ starting from the leaves of the quadtree and proceeding until the root is reached. The expression in Eq. (7) involves the class-conditional PDF $p(y_s|x_s)$ of each observation y_s conditioned to the related label x_s, the prior probability $P(x_s)$ of each label x_s and the transition probability $P(x_s|x_{s^-})$ of the label of each site s from the label of the parent site s^-. The class-conditional PDFs are estimated through the procedure discussed in Sec. 2.2. We refer to Secs. 3.3 and 3.4 for the estimations of the transition and prior probabilities, respectively.

The top-down pass in the proposed algorithm is truncated, in the sense that, first, we maximize the posterior marginal only at the root of the quadtree (see Figs. 2 and 3). This means that, first, the MPM criterion is applied to estimate the label x_s of each site at the coarsest scale level, i.e., $s \in S^R$. The resulting classification map is used to estimate the prior probabilities $P(x_s)$ at this level ($s \in S^R$; see Sec. 3.4). Then, for each finer level $n < R$, first, the prior-probability distribution is derived as a function of the prior-probability distribution at the parent level and of the transition probabilities from the parent to the current level, i.e.:

$$P(x_s) = \sum_{x_{s^-} \in \Omega} P(x_s|x_{s^-})P(x_{s^-}) \quad \forall s \in S^n. \quad (8)$$

Then, the MPM criterion is applied again to a smaller quadtree to estimate the label x_s of each site at the current n-th scale level, i.e., $s \in S^n$. The procedure is repeated until the 0-th scale (i.e., the finest scale) is reached (see Fig. 3). The maximization of $P(x_s|Y)$ is done by employing a modified Metropolis dynamics (MMD) algorithm, that has good properties for both its relatively low computational burden and the accuracy of its results [1].

3.3. Transition probabilities

According to the aforementioned scale-Markovianity property (see Sec. 3.1), the transition probabilities between the scales, $P(x_s|x_{s^-})$, determine the hierarchical structure of the considered MRF because they characterize the causality associated with the statistical interactions between consecutive levels of the quadtree. We model the transition probability in the form introduced by Bouman et al., i.e. ($n = 0, 1, \ldots, R-1$) [11]:

$$P(x_s|x_{s^-}) = \begin{cases} \theta_n, & \text{if } x_s = x_{s^-} \\ \dfrac{1-\theta_n}{M-1}, & \text{otherwise,} \end{cases} \quad \forall s \in S^n. \quad (9)$$

The parameter θ_n associated with the n-th scale has to satisfy the condition $\theta_n > 1/M$. This model favors an identical parent-child labeling. Here, θ_n is chosen independent of the level n (i.e., $\theta_n = \theta$ for all n).

3.4. Prior probabilities

According again to the spatial MRF formulation in Sec. 3.1, also the set X^n of the class labels at each n-th scale ($n = 0, 1, \ldots, R$) is an MRF. Specifically, the well-known Potts MRF model is adopted at each scale, i.e. ($s \in S^n$):

$$P(x_s|x_t, t \in S^n, t \sim s) \propto \exp\left[-\beta \sum_{s \sim t} \delta(x_s, x_t)\right], \quad (10)$$

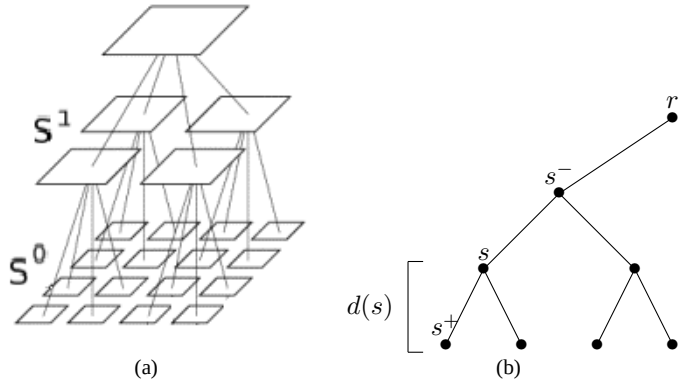

Fig. 1. (a) Hierarchical model structure: quad-tree; (b) Quad-tree notations.

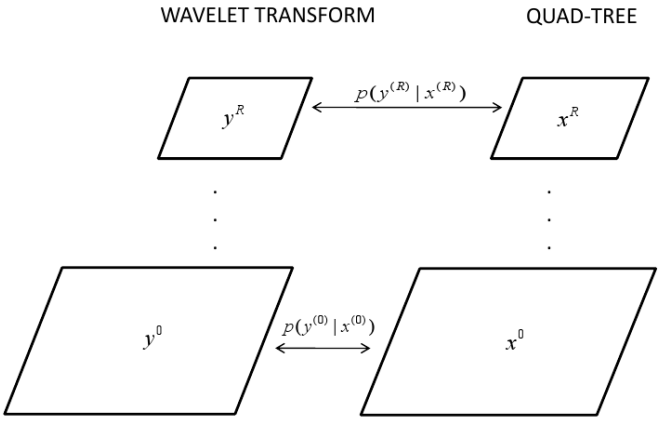

Fig. 2. Generic hierarchical graph-based model of the quad-tree.

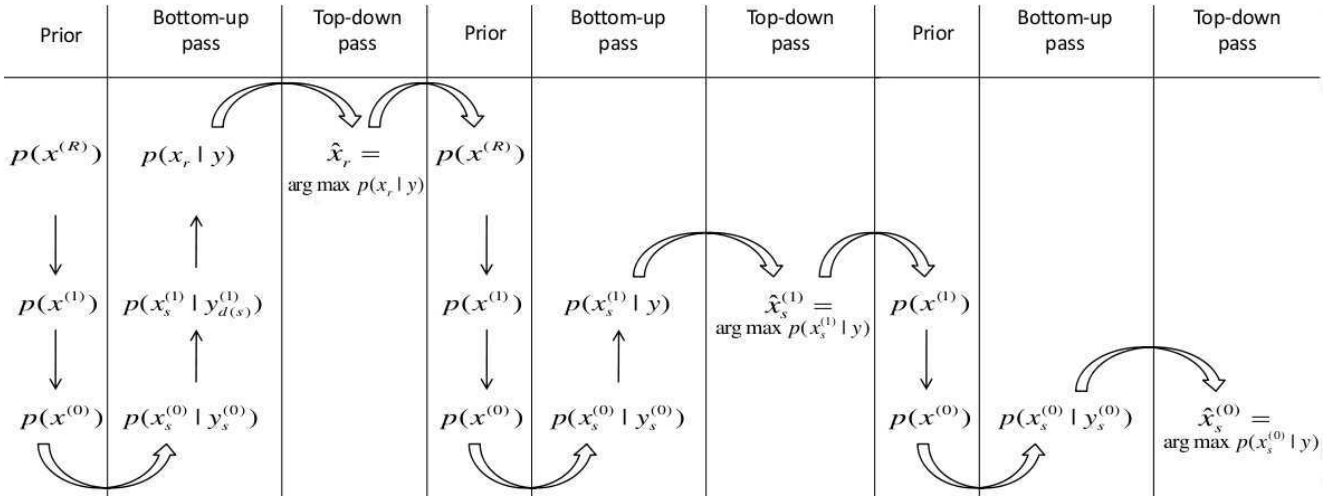

Fig. 3. Proposed MPM estimation on the quadtree represented in Fig. 2. In this example, $R = 2$. For the sake of clarity, the involved scale levels are highlighted with the superscript (n) ($n = 0, 1, 2$).

where $\delta(\cdot)$ denotes the Kronecker symbol (i.e., $\delta(a,b)=1$ for $a=b$ and $\delta(a,b)=0$ otherwise). In the proposed method, to estimate the priors given the current classification map, we replace the prior probability $P(x_s)$ by the local conditional prior probability in Eq. (10). This choice generally provides a biased prior-probability estimate, but favors spatial adaptivity, a desired property when working with VHR images in which spatial details are usually apparent. Furthermore, for the same reason, instead of using a classical second-order neighborhood composed just of the 8 pixels surrounding a given site, we consider different kinds of set geometries to define the neighborhood of each pixel and we separately select, for each site, the one that leads to the smallest energy (adaptive neighborhood). The adaptivity of the neighborhood aims to take into account the geometrical properties of the different areas in our original image. Details can be found in [17].

4. EXPERIMENTAL RESULTS

We present results obtained on a single-pol COSMO-SkyMed image of the quay of Port-au-Prince (Haiti) (©ASI, 2009), HH polarization, StripMap acquisition mode (2.5-m pixel spacing), geocoded, single-look image, 920×820 pixels, shown in Fig. 4(a). Based on preliminary experiments (not reported for brevity), a 5×5 window was used for texture extraction through GLCM. This choice provided more accurate results on the considered data set than other window sizes ranging in $[3; 17]$. Windows larger than 17×17 have not been considered to prevent smearing or oversmoothing effects on object edges. The proposed method was applied with Daubechies-10 wavelets [3]. We empirically selected this wavelet operator because it reported the highest classification accuracy compared to other families (details can be found in [17]).

Spatially disjoint training and test sets were build by visual image interpretation. The considered classes were "water," "urban areas," and "vegetation." The following classification methods were experimentally compared:

1. The proposed amplitude-texture multiscale MPM-based approach.
2. The proposed multiscale MPM-based approach applied solely to the SAR amplitude feature (no texture).
3. The previous multiscale MRF-based approach by Laferte et al. [11], which is based solely on the SAR amplitude feature (no texture).
4. The previous amplitude-texture single-scale approach in [10] which is based on the PDF estimation method described in Sec. 2 and on a (non-hierarchical) Potts MRF (in this case, β was set to 1.2).

Laferte's algorithm was applied to a quadtree generated as in the case of the proposed method, and the related prior probabilities at the root were estimated by using a k-nearest neighbor (k-NN) preliminary classification, with k obtained through cross-validation [2]. Preliminary experiments (not reported for brevity) suggested that the proposed method obtained the highest accuracy when applied with $R=2, \beta=4.8$, and $\theta=0.8$.

The results obtained by the proposed method were satisfying: the classification map was visually quite detailed (see Fig. 4(c)) and the overall accuracy was 98.07% (see Table 1). As expected, the hierarchical model allowed taking properly into account spatial details and was also remarkably robust against speckle. Moreover, the urban areas were well discriminated through the use of the textural information in the appropriate copula-based model. The improvement granted by the use of textures is highlighted by the comparison with the results obtained when applying the proposed method to only the amplitude SAR image (see Figs. 4 (c) and (d)).

To isolate the improvements brought by the proposed hierarchical model, we compared it with the previous Laferte's method, by focusing for both methods only on the SAR amplitude feature. The proposed method was less affected by speckle (see Fig. 4) thanks to the proposed prior update algorithm, especially in the case of the "vegetation" class (see the top center of the maps). Moreover, the classification accuracy for "urban" was higher with the developed method than with Laferte's technique that erroneously classified almost all roads as vegetation (see, e.g., the bottom center of Fig. 4(e)).

By looking at Table 1, we remark that slightly higher accuracies were obtained on the test set by the single-scale MRF-based approach (see Fig. 4(f)). Nevertheless, we point out that this result was obtained at the expense of quite a strong smearing effect on object borders. This effect does not influence the classification accuracies in Table 1 because, as usual in remote sensing, test pixels were located inside homogeneous image regions, i.e., no test pixels were available at the spatial edges. Thus, the hierarchical approach turned out to be preferable for the classification of urban areas because it allowed spatially more precise details to be extracted as compared to the single-scale method. In general, the main misclassifications for "water" derived from the cross-like artifact of SAR acquisition (point spread function of the SAR sensor [15]). None of the algorithms employed in this comparison was robust to this artifact.

The experiments were conducted on an Intel Xeon quad-core (2.40 GHz, 12-MB cache), 18-GB RAM, 64-bit Linux system. The proposed algorithm ran in 6 minutes and 45 seconds, an acceptable time as compared to Laferte's method, which took 5 minutes and 30 seconds, given the visual aforementioned improvement in the classification map.

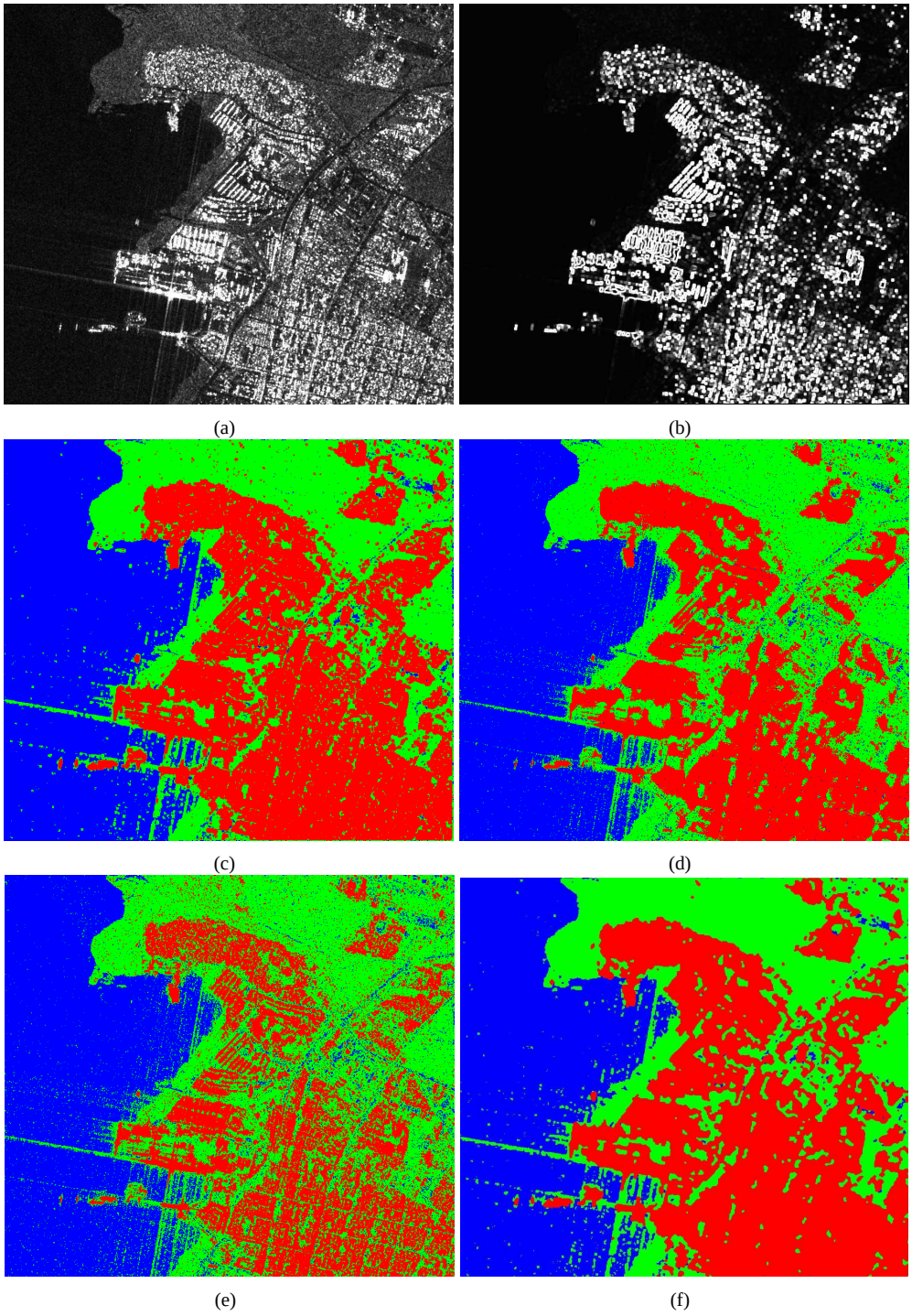

Fig. 4. Port-au-Prince data set. SAR input image (a) and its extracted textural feature (b). Classification maps (water in blue, urban areas in red and vegetation in green) obtained applying different methods: amplitude-texture statistics combined with the hierarchical method proposed in this paper (c), hierarchical method proposed in this paper based on solely amplitude data (d), hierarchical Laferte's method based on amplitude data (e), amplitude-texture statistics combined with a single-scale MRF model (f).

5. CONCLUSION

The supervised classification method proposed in this paper combines a joint copula-based model for the statistics of SAR amplitude data and extracted textural features, and a multiscale hierarchical Markov random field that integrates a case-specific prior probability update technique

Table 1. Accuracy for each of the 3 classes and overall results for the test areas of the Port-au-Prince quay.

	Port-au-Prince quay			
	water	urban	vegetation	**overall**
Proposed method	97.65%	97.99%	98.56%	**98.07%**
Proposed method (no texture)	97.67%	97.27%	98.29%	**97.74%**
Laferte (no texture)	97.61%	88.52%	96.74%	**94.29%**
MRF-based classif.	97.59%	99.03%	99.28%	**98.63%**

aimed at improving robustness against speckle. The class labels are estimated by resorting to a non-iterative optimization algorithm based on the MPM criterion. The experimental results generated by the proposed hierarchical classification algorithm when applied to VHR COSMO-SkyMed data appeared to be a good trade-off between the quite oversmoothed results produced by a single-scale MRF-based method and the rather noisy map obtained by using a previous multiscale MRF-based method. Furthermore, the developed approach could be further extended to the use of multi-polarization, multi-resolution, and/or multi-sensor data, which represents a crucial advantage given the considerable amount of remotely sensed data acquired on a daily basis by current VHR sensors. This is considered as the main direction of further research.

6. ACKNOWLEDGMENT

The work of A. Voisin was supported in part by the Direction Générale de l'Armement (DGA, France) and by the Institut National de Recherche en Informatique et Automatique (INRIA, France). The authors would like to thank Dr. M. De Martino (University of Genoa, Italy) for preparing the ground truth maps, and the Italian Space Agency for providing the COSMO-SkyMed (CSK®) image (COSMO-SkyMed Product - ©ASI - Agenzia Spaziale Italiana - 2009. All Rights Reserved) in the framework of the project "Development and validation of multitemporal image analysis methodologies for multirisk monitoring of critical structures and infrastructures (2010-2012)."

7. REFERENCES

[1] M. Berthod, Z. Kato, S. Yu, and J. Zerubia. Bayesian image classification using Markov random fields. *Image and Vision Computing*, 14(4):285–295, 1996.

[2] C. M. Bishop. *Pattern Recognition and Machine Learning*. Springer-Verlag, New-York, 2006.

[3] I. Daubechies. Orthonormal bases of compactly supported wavelets. *Communications on Pure and Applied Mathematics*, 41(7):909–996, 1988.

[4] S. Dellepiane, D. D. Giusto, S. B. Serpico, and G. Vernazza. SAR image recognition by integration of intensity and textural information. *Int. J. Remote Sens.*, 12(9):1915–1932, 1991.

[5] J. Feng, L. Jiao, X. Zhang, and D. Yang. Bag-of-visual-words based on clonal selection algorithm for SAR image classification. *IEEE Geosci. Remote Sens. Lett.*, 8(4):691–695, 2011.

[6] S. Geman and D. Geman. Stochastic relaxation, Gibbs distributions, and the Bayesian restoration of images. *IEEE Trans. Pattern Anal. Mach. Intell.*, 6(6):721–741, 1984.

[7] C. Graffigne, F. Heitz, P. Perez, F. Preteux, M. Sigelle, and J. Zerubia. Hierarchical Markov random field models applied to image analysis: a review. In *Proc. SPIE Conf. on Neural, Morphological and Stochastic Methods in Image Proc.*, volume 2568, pages 2–17, 1995.

[8] R. M. Haralick, K. Shanmugam, and I. Dinstein. Textural features for image classification. *IEEE Trans. Syst., Man, Cybern.*, 3(6):610–621, 1973.

[9] D. Huard, G. Evin, and A.-C. Fabre. Bayesian copula selection. *Comput. Statist. Data Anal.*, 51(2):809–822, 2006.

[10] V. Krylov, G. Moser, S. B. Serpico, and J. Zerubia. Supervised high resolution dual polarization SAR image classification by finite mixtures and copulas. *IEEE J. Sel. Top. Signal Proc.*, 5(3):554–566, 2011.

[11] J.-M. Laferte, P. Perez, and F. Heitz. Discrete Markov modeling and inference on the quad-tree. *IEEE Trans. Image Process.*, 9(3):390–404, 2000.

[12] S. G. Mallat. *A wavelet tour of signal processing*. Academic Press, 3rd edition, 2008.

[13] G. Moser, S. B. Serpico, and J. Zerubia. Dictionary-based Stochastic Expectation Maximization for SAR amplitude probability density function estimation. *IEEE Trans. Geosci. Remote Sens.*, 44(1):188–199, 2006.

[14] R. B. Nelsen. *An introduction to copulas*. Springer, New York, 2nd edition, 2006.

[15] C. Oliver and S. Quegan. *Understanding Synthetic Aperture Radar images*. SciTech Publishing, 2004.

[16] M. Silveira and S. Heleno. Separation between water and land in SAR images using region-based level sets. *IEEE Geosci. Remote Sens. Lett.*, 6(3):471–475, 2009.

[17] A. Voisin, V. Krylov, G. Moser, S. B. Serpico, and J. Zerubia. Classification of very high resolution SAR images of urban areas. Research report 7758, INRIA, France, oct 2011.

[18] A. Voisin, G. Moser, V. Krylov, S. B. Serpico, and J. Zerubia. Classification of very high resolution SAR images of urban areas by dictionary-based mixture models, copulas and Markov random fields using textural features. In *Proc. of SPIE Symposium on Remote Sensing 2010*, volume 7830, page 78300O, Toulouse, France, Sept. 2010.